American Mineralogist, Volume 62, pages 67–78, 1977

An X-ray and neutron diffraction study of hydrous low cordierite

JANET P. COHEN,[1] FRED K. ROSS[2] AND G. V. GIBBS

Virginia Polytechnic Institute and State University
Blacksburg, Virginia 24061

Abstract

The structure of low cordierite, $(Na_{0.05}K_{0.02}Ca_{0.02})$ $(Mn_{0.01}Mg_{1.91}Fe_{0.08})(Si_{5.01}Al_{3.95}O_{18.01})(H_2O)_{0.56}$; a = 17.079(3), b = 9.730(2), c = 9.356(2) Å; *Cccm*, from White Well, Australia (Pryce, 1973), was refined by least-squares methods using X-ray and neutron diffraction data. A site-refinement with the neutron data indicates an ordered arrangement of Al and Si in the tetrahedral framework. Neutron $\Delta\rho$ maps calculated around the point at (0,0,1/4) indicate that the H_2O molecules in the cavity at z = 1/4 are disordered into four different orientations with the H–O–H plane of each nearly parallel to (001). This result disagrees with the possible orientation parallel to (100) proposed from infrared absorption spectra and confirmed by an NMR study. A neutron site refinement showed no evidence for substitution of H^+ for Al and Si in the tetrahedral framework, and a $\Delta\rho$ map calculated over the whole unit cell shows no residual negative peaks that may be ascribed to H^+. The alkaline atoms are centered about (0,0,0). Mulliken population analyses calculated for the tetrahedral framework using constant bond lengths and the observed angles within and between the tetrahedral ions indicate that the bond length variations in the framework may be ordered in terms of bonding and antibonding Mulliken overlap populations. As expected, the bond length variations in the framework correlate linearly (r = 0.9) with the valence angles within and between the tetrahedra. Calculations for 4-membered $Al_2Si_2O_{12}$ rings like those in cordierite result in a lower electronic energy when Al- and Si-containing tetrahedra alternate than when "the aluminum avoidance rule" is violated. Calculations for the 6-membered $Al_2Si_4O_{18}$ rings like those in cordierite predict a higher energy when AlO_4 tetrahedra are adjacent, but predict identical energies when the two AlO_4 tetrahedra are separated by one or two SiO_4 tetrahedra.

Introduction

The location and the role of water in cordierite, $(Mg,Fe,Mn)_2Al_4Si_5O_{18}\cdot nH_2O$, has been the subject of considerable study and debate in the last few years (Smith and Schreyer, 1960; Schreyer and Yoder, 1964; Newton, 1966, 1972). According to Sugiura (1959) and Iiyama (1960), there are two types of water in cordierite. Evidence for this was obtained in heating experiments, from which they proposed that a gradual weight loss below 500°C represents a loss of loosely bound molecular H_2O from the channels, whereas a rapid weight loss above 500°C represents a loss of water replacing silicate tetrahedra by one of three possible substitutions: $O^{-2} \rightarrow 2(OH)^-$; $SiO_4 \rightarrow 4(OH)^-$; or $Si^{+4} \rightarrow 4H^+$. However, no evidence for this type of substitution was observed in a later study using infrared absorption spectroscopy (Schreyer and Yoder, 1964). On the other hand, evidence for molecular H_2O in the channels has been provided by broad low maxima centered at (0,0,1/4) in electron density maps of hydrous cordierite (Gibbs, 1966; Meagher, 1967). An X-ray determination of the orientation of the H_2O molecule within the channel is difficult because hydrogen atoms are poor scatterers of X-rays. Therefore, Farrell and Newnham (1967) resorted to infrared absorption spectroscopy to determine a possible orientation of the water molecule in the (100) of the Guilford cordierite with the H–H vector parallel to [001]. This orientation was later confirmed in a nuclear magnetic resonance study of a cordierite from Madagascar (Tsang and Ghose, 1972).

The present X-ray and neutron diffraction study of

[1] Present address: Union Carbide Corporation, Tarrytown, New York.

[2] Argonne National Laboratory C.E.A. Participant, 1973 and 1974.

hydrous Mg-rich low cordierite (Cohen, 1975; Cohen *et al.* 1975) was undertaken to determine (1) the location and orientation of the water molecule in the channel, (2) whether H^+ substitutes for Al and Si in tetrahedral coordination, (3) the degree of Al/Si order in the tetrahedral framework, and (4) whether the steric details and the ordered configuration of Al and Si in the tetrahedral framework may be rationalized in terms of semi-empirical molecular orbital theory.

Experimental

The pale-blue translucent cordierite crystals used in this study were kindly supplied by M. W. Pryce, who described their occurrence in a phlogopite schist near White Well, Western Australia. The chemical formula of this cordierite, here called the White Well corderite, is

$$(Na_{0.05}K_{0.02}Ca_{0.02})(Mn_{0.01}Mg_{1.91}Fe_{0.08})(Si_{5.01}Al_{3.95}O_{18.01})(H_2O)_{0.56},$$

$Z = 4$ (Pryce, 1973), being close to the end-member composition of the Mg–cordierite. Since Be was not listed in Pryce's chemical analysis, an emission spectroscopic analysis was undertaken because Be is a common constituent in many cordierites. The analysis, completed by courtesy of the Union Carbide Central Scientific Laboratories at Tarrytown, New York, showed the White Well cordierite to contain no Be. The cell parameters and the distortion indices of the cordierite determined by least-squares refinement of X-ray and neutron diffraction data are compared with those determined by Pryce as follows:

	Pryce (1973)	Neutron study	X-ray study
a	17.055(5)	17.086(10)	17.079(3)
b	9.724(5)	9.737(6)	9.730(2)
c	9.350(1)	9.356(6)	9.356(2)
Δ	0.23°	0.24°	0.25°

The cell parameters obtained in the least-squares analysis of X-ray data were considered most precise and were used in all subsequent calculations. The density, 2.56 g/cm^3, calculated from the observed cell parameters and composition compares well with that [2.57(1)] measured by Pryce (1973). The refractive indices, $\alpha = 1.536$, $\beta = 1.540$, $\gamma = 1.543$, and the optic axial angle, $2V_\alpha = 80°$, were measured using plane polarized white light (Pryce, 1973). Precession photographs of the White Well cordierite (MoK_α radiation) confirm the space group *Cccm* for cordierite as determined by Byström (1942).

The reader is referred to Cohen (1975) for a discussion of the experimental procedures used in recording the neutron and X-ray diffraction data, for a listing of the observed and calculated structural amplitudes, and for an interpretation of the $\Delta\rho$ maps used in determining the orientation of the water molecules in the channel. The final positional and thermal parameters are given in Table 1; the interatomic distances and angles are given in Tables 2, 3 and 4; and the orientations and magnitudes of the root mean square (r.m.s.) displacements are given in Table 5.

Table 1. Final fractional coordinates and thermal parameters ($\times 10^5$) of the White Well cordierite

Atom	x		y		z		β_{11}		β_{22}		β_{33}		β_{12}		β_{13}		β_{23}	
	N*	X**	N	X	N	X	N	X	N	X	N	X	N	X	N	X	N	X
$T_1 1$	1/4		1/4		0.2507(3)	0.2502(1)	52(4)	57(3)	109(14)	133(8)	148(20)	110(9)	13(7)	15(3)	0		0	
$T_1 6$	0		1/2		1/4		43(5)	39(3)	202(18)	146(10)	174(24)	98(10)	0		0		0	
$T_2 1$	0.1926(1)	0.1926(1)	0.0780(2)	0.0778(1)	0		33(4)	38(2)	104(11)	83(7)	201(18)	118(8)	3(6)	7(3)	0		0	
$T_2 6$	.0508(1)	.0508(1)	.3081(2)	.3079(1)	0		39(5)	31(3)	124(14)	121(8)	154(21)	132(9)	2(7)	8(3)	0		0	
$T_2 3$	-.1352(1)	-.1352(1)	.2372(2)	.2375(1)	0		38(4)	37(2)	119(12)	99(7)	168(18)	105(8)	9(5)	-11(3)	0		0	
$O_1 1$	.2473(1)	.2474(1)	.1028(1)	.1029(1)	.1422(1)	.1410(2)	73(2)	74(5)	160(6)	153(13)	253(9)	179(15)	10(3)	9(5)	-32(4)	-31(6)	-13(7)	-19(11)
$O_1 6$	.0623(1)	.0620(1)	.4161(1)	.4160(2)	.1512(1)	.1512(2)	52(2)	54(5)	214(6)	211(13)	231(9)	180(15)	9(3)	17(6)	-7(4)	-2(6)	-75(7)	-71(11)
$O_1 3$	-.1733(1)	-.1732(1)	.3103(1)	.3101	.1416(1)	.1416(2)	65(2)	54(4)	206(6)	202(14)	231(9)	199(15)	-17(3)	-11(6)	27(4)	20(6)	-61(8)	-29(11)
$O_2 1$	.1222(1)	.1223(1)	.1844(1)	.1839(2)	0		70(3)	70(7)	242(10)	248(21)	437(17)	386(25)	61(5)	51(9)	0		0	
$O_2 6$	-.0432(1)	-.0430(1)	.2478(1)	.2476(2)	0		41(3)	53(7)	336(11)	301(21)	410(16)	330(24)	-26(5)	-27(9)	0		0	
$O_2 3$	-.1646(1)	-.1645(1)	.0796(1)	.0792(2)	0		93(3)	91(7)	133(9)	144(19)	421(16)	361(23)	-32(5)	-37(9)	0		0	
M	.1626(1)	.1625(1)	1/2		1/4		38(3)	48(3)	165(9)	142(9)	212(14)	181(9)	0		0		5(11)	0(7)
Ow	0.0270		0		1/4		9.8											
A&k***	0		0		0		5.0											
H1	-.0291		-0.0412		0.2397		5.0											
H2	.0174		.0833		.3050		5.0											

* Neutron diffraction data

** X-ray diffraction data

*** A&k = 0.05 Na + 0.02 K + 0.02 Ca

Table 2. Interatomic distances [Å($\hat{\sigma}$)] and angles [($\hat{\sigma}$)] in White Well cordierite

Atoms		Neutron Distance	Neutron Angle at metal atom	X-ray Distance	X-ray Angle at metal atom
$T_1$1-$O_1$1*	[2]**	1.761(2)		1.760(2)	
$T_1$1-$O_1$3'	[2]	1.754(2)		1.757(2)	
Mean		1.758(1)		1.758(1)	
$O_1$3''-$O_1$3'	[1]	2.871(2)	109.8(2)	2.873(3)	109.6(1)
$O_1$1-$O_1$3''	[2]	2.586(2)	94.7(1)	2.587(2)	94.7(1)
$O_1$1-$O_1$3'	[2]	3.131(2)	125.9(1)	3.132(2)	125.9(1)
$O_1$1-$O_1$1'	[1]	2.866(2)	108.9(2)	2.864(3)	109.0(1)
Mean		2.862(1)	110.0(1)	2.862(1)	110.0(1)
$T_1$6-$O_1$6	[4]	1.628(1)		1.626(2)	
Mean		1.628(1)		1.626(2)	
$O_1$6-$O_1$6'	[2]	2.818(2)	119.8(1)	2.813(3)	119.7(1)
$O_1$6-$O_1$6'''	[2]	2.682(2)	110.8(1)	2.676(3)	110.7(1)
$O_1$6-$O_1$6''	[2]	2.466(2)	98.4(1)	2.467(3)	98.7(1)
Mean		2.655(1)	109.7(1)	2.652(1)	109.7(1)
$T_2$1-$O_1$1	[2]	1.636(1)		1.636(2)	
$T_2$1-$O_2$1	[1]	1.586(2)		1.583(2)	
$T_2$1-$O_2$3'	[1]	1.606(2)		1.601(2)	
Mean		1.616(1)		1.614(1)	
$O_1$1-$O_1$1m	[1]	2.642(2)	107.7(1)	2.638(3)	107.4(1)
$O_1$1-$O_2$1	[2]	2.634(2)	109.6(1)	2.632(2)	109.7(1)
$O_1$1-$O_2$3'	[2]	2.625(1)	108.1(1)	2.624(2)	108.3(1)
$O_2$1-$O_2$3'	[1]	2.669(2)	113.4(1)	2.659(3)	113.3(1)
Mean		2.638(1)	109.4(1)	2.635(1)	109.4(1)
$T_2$3-$O_1$3	[2]	1.639(1)		1.636(2)	
$T_2$3-$O_2$6	[1]	1.574(2)		1.578(2)	
$T_2$3-$O_2$3	[1]	1.614(2)		1.619(2)	
Mean		1.616(1)		1.617(1)	
$O_1$3-$O_1$3m	[1]	2.650(2)	107.9(1)	2.649(3)	108.2(1)
$O_1$3-$O_2$6	[2]	2.657(2)	111.6(1)	2.659(2)	111.6(1)
$O_1$3-$O_2$3	[2]	2.610(2)	106.8(1)	2.613(2)	106.8(1)
$O_2$6-$O_2$3	[1]	2.641(2)	111.9(1)	2.644(3)	111.5(1)
Mean		2.638(1)	109.4(1)	2.640(1)	109.4(1)
$T_2$6-$O_1$6	[2]	1.773(2)		1.773(2)	
$T_2$6-$O_2$6	[1]	1.710(2)		1.706(2)	
$T_2$6-$O_2$1	[1]	1.714(2)		1.716(2)	
Mean		1.742(1)		1.742(1)	
$O_1$6-$O_1$6m	[1]	2.829(2)	105.8(1)	2.829(3)	105.8(1)
$O_1$6-$O_2$6	[2]	2.816(1)	107.9(1)	2.812(2)	107.8(1)
$O_1$6-$O_2$1	[2]	2.852(2)	109.7(1)	2.856(2)	109.9(1)
$O_2$1-$O_2$6	[1]	2.892(2)	115.3(1)	2.890(3)	115.2(1)
Mean		2.843(1)	109.4(1)	2.842(1)	109.4(1)
M-$O_1$6	[2]	2.111(1)		2.113(2)	
M-$O_1$1'	[2]	2.099(1)		2.100(2)	
M-$O_1$3'	[2]	2.114(1)		2.115(2)	
Mean		2.108(1)		2.109(1)	
$O_1$6-$O_1$6''	[1]	2.446(2)	71.5(1)	2.467(3)	71.4(1)
$O_1$6-$O_1$3'	[2]	2.900(1)	86.7(1)	2.902(2)	86.7(1)
$O_1$6''-$O_1$3'	[2]	3.269(1)	101.4(1)	3.272(2)	101.4(1)
$O_1$1''-$O_1$6''	[2]	3.259(1)	101.4(1)	3.261(2)	101.4(1)
$O_1$3'-$O_1$1'	[2]	2.586(2)	75.7(1)	2.587(2)	75.7(1)
$O_1$3'-$O_1$1''	[2]	3.153(1)	96.9(1)	3.155(2)	96.9(1)
$O_1$1''-$O_1$1'	[1]	2.855(2)	85.7(1)	2.858(3)	85.8(1)
Mean		3.000(1)	90.1(1)	2.973(1)	90.1(1)

* For nomenclature see Fig. 1.

** Multiplicity of bond.

Nomenclature

The labels assigned to the T and O atoms in the White Well cordierite follow a scheme designed to facilitate a comparison between the crystal structures of the hexagonal and orthorhombic polymorphs of cordierite (Meagher and Gibbs, in preparation). The subscript of each atom label given in Tables 1–5 and in the upper quarter of Figure 1 identifies those atoms that are equivalent in hexagonal cordierite T_1 = {$T_1$1,$T_1$6}, T_2 = {$T_2$1,$T_2$6,$T_2$3}, O_1 = {$O_1$1,$O_1$6,$O_1$3} and O_2 = {$O_2$1,$O_2$6,$O_2$3}, whereas the third symbol of each atom label denotes the symmetry operation (1 = identity map, 6 = sixth-turn, 3 = third-turn) that relates the atoms in the equivalent sets. For example, the identity symbol, 1, is attached to the atom labels of hexagonal cordierite T_1, T_2, O_1, and O_2 to denote that $T_1$1, $T_2$1, $O_2$1, and $O_2$1 are related to T_1, T_2, O_1, and O_2 by the identity mapping. Similarly, the sixth-turn symbol, 6, is attached to the labels T_1, T_2, O_1, and O_2 to denote that $T_1$6, $T_2$6, $O_1$6, and $O_2$6 are related to T_1, T_2, O_1, and O_2 by a sixth-turn. Finally, the symbol for a third-turn, 3, is attached to the labels to denote that $T_2$3, $O_1$3, and $O_2$3 are related to T_2, O_1, and O_2 by a third-turn. In terms of this nomenclature, the labels used by Gibbs (1966) for the T and O atoms of low cordierite correspond as follows: $T_1$1 = T_1; $T_1$6 = T_2; $T_2$1 = T_3; $T_2$6 = T_5; $T_2$3 = T_4; $O_1$1 = O1; $O_1$6 = O2; $O_1$3 = O3; $O_2$1 = O5; $O_2$6 = O4; $O_2$3 = O6.

Table 3. Nearest neighbor cation-cation distances and interatomic angles at oxygen atoms

		N		X	
		Distance between cations	Angle at oxygen atom	Distance between cations	Angle at oxygen atom
Six-membered rings					
$T_2 1$-$O_2 1$-$T_2 6$*	[2]**	3.298(2)	176.1(1)	3.298(1)	176.0(2)
$T_2 1$-$O_2 3'$-$T_2 3$	[2]	3.220(2)	179.1(1)	3.220(1)	179.5(2)
$T_2 3$-$O_2 6$-$T_2 6$	[2]	3.250(2)	163.7(1)	3.250(1)	163.5(2)
Mean		3.256(1)	173.0(1)	3.256(1)	173.0(1)
Four-membered rings					
$T_1 6$-$O_1 6$-$T_2 6$	[2]	3.116(1)	132.6(1)	3.117(1)	132.9(1)
$T_1 1$-$O_1 1$-$T_2 1$	[2]	3.044(2)	127.2(1)	3.042(1)	127.2(1)
$T_1 1$-$O_1 3$-$T_2 3$	[2]	3.050(2)	128.0(1)	3.053(1)	128.2(1)
Mean		3.070(1)	129.3(1)	3.071(1)	129.4(1)
Octahedron					
$T_2 1$-$O_1 1$-M	[2]	3.488(2)	137.7(1)	3.488(2)	137.7(1)
$T_1 1$-$O_1 1$-M	[2]	2.854(1)	94.9(1)	2.855(1)	95.0(1)
$T_2 3$-$O_1 3$-M	[2]	3.497(2)	137.1(1)	3.495(2)	137.0(1)
$T_1 1$-$O_1 3$-M	[2]	2.854(1)	94.6(1)	2.855(1)	94.5(1)
$T_2 6$-$O_1 6$-M	[2]	3.550(1)	131.9(1)	3.550(1)	131.8(1)
$T_1 6$-$O_1 6$-M	[2]	2.777(2)	95.0(1)	2.777(2)	94.9(1)
Mean		3.170(1)	115.2(1)	3.170(1)	115.2(1)

* For nomenclature see Fig. 1.

** Multiplicity of bond.

Discussion

Basic structure and classification of cordierite

The present study confirms the basic structure of cordierite proposed by Gossner and Mussgnug (1928), Takane and Takeuchi (1936), and Byström (1942), and the order configuration of Al- and Si-rich tetrahedra in low cordierite determined by Gibbs (1966). The structure may be viewed as a tetrahedral framework consisting of chains of 4-membered rings of alternating AlO_4 and SiO_4 tetrahedra cross-linked into 6-membered rings of $Al_2Si_4O_{18}$ composition [See Fig. 1; see also Gibbs' (1966) Fig. 7]. The *M*-atoms (Mg,Fe,Mn) are located in the framework in slightly flattened octahedra that share three edges, two with AlO_4 tetrahedra and one with a SiO_4 tetrahedron. When present, H_2O occurs as zeolitic water in the large cavities formed between the 6-membered rings (Smith and Schreyer, 1960; Gibbs, 1966; Meagher, 1967), whereas alkaline atoms occur at the center of the ring (Meagher, 1967). According to Zoltai (1960), cordierite should be classified as a framework silicate because its SiO_4 and AlO_4 tetrahedra share corners in perfect alternation throughout the structure with SiO_4 tetrahedra sharing corners in the 6-membered ring. Zoltai's classification has since been borne out by structural analyses of cordierite, which indicate that the polymorphism of cordierite involves all the tetrahedral atoms in the structure rather than just those in the 6-membered ring as previously believed. Nevertheless, Strunz *et al.* (1971) continue to classify cordierite as a ring silicate because they believe that its cation-containing octahedra disqualify it as a "real framework or tecto-silicate such as feldspar in its various forms." If we accept their rule then the feldspar anorthite, which also contains cation-filled octahedra (Phillips *et al.*, 1973), should also be disqualified as a framework silicate. Their rule appears to be inconsistent and we urge that they reconsider their classification of cordierite.

Si–Al ordering in the tetrahedral framework

Gibbs (1966) has concluded from the individual mean tetrahedral *T*–O bond lengths, ⟨*T*–O⟩, and the

Table 4. Approximate interatomic distances (Å) of channel atoms*

Atoms	Distance
H1(1)-$O_2$6	3.26
-$O_2$1	3.08
-$O_2$3	3.38
H2(1)-$O_2$6	2.47
-$O_2$1	3.16
-$O_2$3	3.11
H1(1)-OW(1)	1.04
H2(1)-OW(1)	0.97
H1(1)-H2(1)	1.57
NaKCa-OW	2.38
-H1(1)	2.33
-H1(2)	2.52
-H2(1)	2.02
-H2(2)	2.98
-$O_2$6	2.52
-$O_2$1	2.75
-$O_2$3	2.92
-$T_2$1	3.38
-$T_2$3	3.26
-$T_2$6	3.12

* For numbering system see Fig. 8.

Bragg-Williams equation for predicting long-range order that the Guilford cordierite is about 90 percent ordered. A neutron tetrahedral site refinement of the White Well cordierite shows it to be completely ordered within the statistical error. Since the $\langle T\text{–}0\rangle$ for the Guilford and the White Well cordierites are statistically identical, we may conclude that both cordierites are completely ordered within the experimental error.

To determine whether the ordered configuration of Al and Si in low cordierite may be rationalized in terms of semiempirical molecular orbital theory, calculations of the total Hückel electronic energies were completed for all possible ordered configurations of AlO_4 and SiO_4 tetrahedra in 4-membered rings of $Al_2Si_2O_{12}$ composition and 6-membered rings of $Al_2Si_4O_{18}$ composition, assuming ideal geometries (Fig. 2). Calculations for the 4-membered rings (like those paralleling c of cordierite) result in a lower electronic energy, implying a more stable configuration, when AlO_4 and SiO_4 tetrahedra alternate (case 1a) than when AlO_4 tetrahedra are adjacent and share a common oxygen (case 2a). This result agrees with the aluminum avoidance rule proposed by Loewenstein (1954) and by Goldsmith and Laves (1955). Calculations for 6-membered rings like those in cordierite resulted in practically identical electronic energies when the AlO_4 tetrahedra in the ring are separated either by one (case 1b) or by two (case 2b) silicate tetrahedra. In agreement with the aluminum avoidance rule, adjacent corner-sharing AlO_4 tetrahedra (case 3b) result in a higher energy, less stable configuration. In an attempt to rationalize low cordierite's preference for the configuration similar to case 1b in terms of electrostatic considerations, the Coulombic attractive potential between all atoms in the $Al_2Si_4O_{18}$ ring for cases 1b and 2b was calculated using the electric charges provided by the EHMO calculations. However, identical values resulted, suggesting that the observed configuration may not be predicted in terms of total Hückel electronic energies or Coulombic potentials for ideal geometries.

Mulliken population analysis for the atoms of tetrahedral framework

EHMO calculations were also completed for the AlO_4 and SiO_4 tetrahedra in cordierite to learn whether the steric details of the tetrahedral frameworks of the Guilford and the White Well cordierites may be rationalized in terms of tetrahedral bond overlap populations, $n(T\text{–O})$, and geminal nonbonded repulsions, $nb(T\text{–O})$, obtained in a Mulliken population analysis. These calculations were made for $(T_5O_{16})^{n-}$ ions using the procedure outlined by Gibbs *et al.* (1974) and a minimum *sp* basis set of atomic orbitals. All the O–T–O and T–O–T angles were clamped at their observed values, but the T–O bond lengths were clamped at fixed values (1.61 Å for SiO_4 and 1.75 Å for AlO_4 tetrahedra). Clamping the T–O bond lengths at a constant value probably removes the bias of $n(T\text{–O})$ being a direct function of the observed T–O bond lengths. However, since the observed valence angles were assumed in the calculations, the $n(T\text{–O})$ values should reflect the angular distortions impressed on the tetrahedral framework by the nontetrahedral cations to satisfy packing and bonding requirements. The values of $n(T\text{–O})$, $nb(T\text{–O})$ and the electrical charges on oxygen, $Q(\text{O})$, used to prepare our figures are given in Table 6.

The $n(T\text{–O})$ values calculated for the AlO_4 and SiO_4 tetrahedra are plotted against observed Al–O and Si–O bond lengths, $d(T\text{–O})_{obs}$, in Figure 3. As observed for the feldspars, the correlations (r = 0.9) between $d(T\text{–O})_{obs}$ *vs.* $n(T\text{–O})$ are well-developed,

Table 5. Magnitudes and orientations of principal axes of thermal ellipsoids in White Well cordierite

Atom, Axis		rms displacement Å($\hat{\sigma}$) N	X	Angle, in degrees, with respect to $+a(\hat{\sigma})$ N	X	$+b(\hat{\sigma})$ N	X	$+c(\hat{\sigma})$ N	X
$T_1$1	1	0.070(5)	0.070(3)	110(9)	90	20(9)	90	90	0
	2	.081(6)	.076(3)	90	64(5)	90	154(5)	180	90
	3	.090(4)	.095(2)	20(9)	26(5)	70(9)	64(5)	90	90
$T_1$6	1	.079(5)	.066(4)	0	90	90	90	90	0
	2	.088(7)	.076(3)	90	180	90	90	180	90
	3	.098(4)	.084(3)	90	90	0	0	90	90
$T_2$1	1	.068(4)	.062(3)	33(48)	107(7)	123(48)	17(7)	90	90
	2	.072(4)	.072(3)	123(48)	90	146(48)	90	90	180
	3	.094(4)	.076(2)	90	17(7)	90	73(7)	0	90
$T_2$6	1	.075(5)	.065(3)	29(69)	24(9)	119(69)	114(9)	90	90
	2	.078(5)	.076(3)	119(69)	90	150(69)	90	90	180
	3	.083(6)	.078(3)	90	65(9)	90	24(9)	0	90
$T_2$3	1	.070(4)	.064(3)	43(16)	55(7)	133(16)	145(7)	90	90
	2	.080(4)	.068(3)	133(16)	90	137(16)	90	90	0
	3	.086(5)	.078(2)	90	35(7)	90	55(7)	180	90
$O_1$1	1	.086(2)	.079(4)	75(12)	113(12)	165(13)	115(27)	88(12)	145(14)
	2	.092(2)	.086(4)	134(7)	112(13)	102(17)	28(25)	134(3)	106(24)
	3	.117(2)	.112(3)	48(3)	33(5)	81(3)	78(5)	136(3)	120(5)
$O_1$6	1	.082(3)	.073(4)	83(20)	74(11)	136(2)	127(4)	134(6)	138(7)
	2	.087(2)	.088(4)	168(13)	158(10)	89(15)	88(8)	101(14)	112(10)
	3	.118(2)	.113(3)	99(3)	104(6)	134(2)	143(4)	46(2)	57(4)
$O_1$3	1	.084(3)	.082(4)	72(12)	39(14)	126(9)	92(15)	138(3)	129(13)
	2	.091(2)	.091(4)	145(9)	116(17)	124(10)	138(8)	84(9)	120(15)
	3	.120(2)	.107(3)	62(3)	63(6)	65(2)	132(8)	49(2)	53(7)
$O_2$1	1	.076(3)	.082(6)	41(2)	40(5)	131(5)	130(5)	90	90
	2	.127(2)	.124(4)	131(2)	130(5)	139(2)	140(5)	90	90
	3	.139(3)	.131(4)	90	90	90	90	0	0
$O_2$6	1	.075(3)	.084(6)	168(2)	163(5)	102(2)	107(5)	90	90
	2	.129(2)	.121(5)	102(2)	90	12(2)	90	90	180
	3	.135(3)	.123(4)	90	83(5)	90	163(5)	0	90
$O_2$3	1	.074(3)	.075(6)	108(3)	112(5)	162(3)	158(5)	90	90
	2	.121(2)	.121(4)	18(3)	22(5)	108(3)	112(5)	90	90
	3	.137(3)	.126(4)	90	90	90	90	0	0
M	1	.075(3)	.082(3)	180	90	90	0(15)	90	90(15)
	2	.089(3)	.084(3)	90	0	171(18)	90	81(18)	90
	3	.097(3)	.090(2)	90	90	81(18)	90(15)	9(18)	0(15)

shorter bonds tending to involve larger $n(T\text{–O})$ values. Since the observed valence angles were used in the calculation of $n(T\text{–O})$, which in turn correlate with $d(T\text{–O})_{obs}$, it follows that $d(T\text{–O})_{obs}$ should correlate with both $\angle\ T\text{–O–}T$ and $\angle\ \text{O–}T\text{–O}$. To test this assertion a multiple linear regression was calculated for $d(T\text{–O})_{obs}$ as a function of $-1/\cos(\angle\ T\text{–O–}T)$ and $\langle \text{O–}T\text{–O}\rangle_3$, the average of the three O–T–O angles common to the observed T–O bond length. Both of these independent parameters were found to make a significant contribution to the regression sum of squares. The observed T–O bond lengths are plotted against the bond lengths, $d(T\text{–O})_{calc}$, calculated from the regression equations in Figure 4 (r = 0.9). The shorter Si–O and Al–O bonds in low cordierite are observed to involve the two-coordinated oxygen atoms while the longer ones involve the three-coordinated oxygen atoms. As the sum of the valence bond strengths, $\zeta(\text{O})$ (Baur, 1970), to the three-coordinated oxygens is larger than that to the two-coordinated oxygen atoms (Table 6), $\zeta(\text{O})$ correlates with $n(\text{Si–O})$ and $n(\text{Al–O})$ as expected (Fig. 5). Because $\zeta(\text{O})$ may be related to the number of valence electrons shared by an oxygen atom and its coordinating metal atoms, the correlation between $n(\text{Si–O})$ and $n(\text{Al–O})$ *vs.* $\zeta(\text{O})$ is consistent with the claim by Pauling (1960) that his electrostatic valence rule may be rationalized in terms of a model based on covalent bonding. In other words, it appears that part of the electrostatic bond strengths for the Al–O and Si–O bonds may be re-

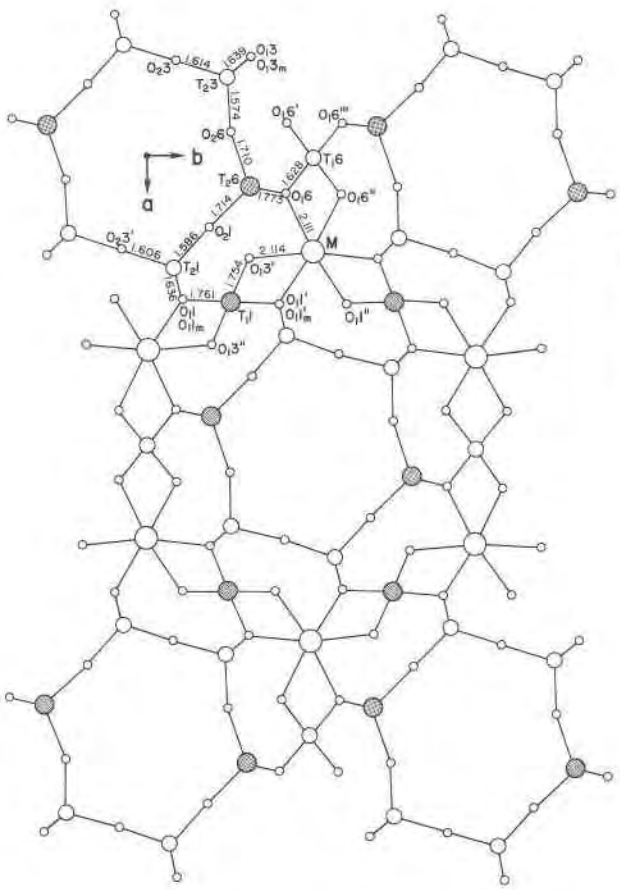

Fig. 1. The crystal structure of low cordierite viewed down the c axis with the T atoms in the 6-membered rings located at $z = 0.0$. The small open circles represent oxygen atoms, the open circles centering M octahedra represent Mg and Fe atoms, the large shaded circles centering the $T_1$1 and $T_2$6 tetrahedra represent Al atoms, and the open circles centering the $T_1$6, $T_2$1, and $T_2$3 tetrahedra represent Si atoms. The nomenclature of the oxygen atoms is given next to the small open circles. The values indicated between atoms refer to selected bond lengths calculated from the neutron diffraction.

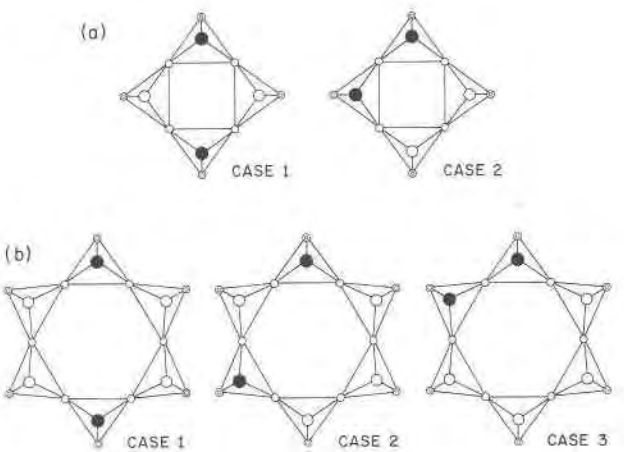

Fig. 2. Drawings of the possible arrangements of AlO_4 and SiO_4 tetrahedral ions in (a) 4-membered rings of $Al_2Si_2O_{12}$ composition (D_{4h} symmetry) and (b) 6-membered rings of $Al_2Si_4O_{18}$ composition (D_{6h} symmetry). The large solid circles represent Al, the large open circles represent Si, the small open circles represent oxygen, and the small double circles represent two oxygen atoms in superposition. Cases 1a and 1b represent configurations topologically identical to those in low cordierite. EHMO calculations predict case 1a to be more stable than 2a and cases 1b and 2b to be of practically identical stability and case 3b to be of significantly lower stability.

flecting some covalent aspect of a bond such as bond overlap population, particularly for bonds having 50 percent or more covalent character.

As stated earlier, the neutron site refinement of the White Well cordierite shows it to be completely ordered within the experimental error. On the other hand, the mean T–O bond lengths, $\langle T$–O$\rangle$, recorded for the Si-containing tetrahedra show the $T_1$6 tetrahedron (1.628 Å) to be significantly larger than $T_2$1 and $T_2$3 (1.616 Å). In light of this evidence, it is tempting to ascribe this larger size to a small amount of Al replacing Si (Smith and Bailey, 1963). However, when the mean bond overlap populations, $\langle n(T$–O$)\rangle$, of these tetrahedra are compared with their $\langle T$–O$\rangle$ values, we see that the $\langle n(T$–O$)\rangle$ value for the $T_1$6 tetrahedron (0.518) is smaller than that calculated for the other two tetrahedra (0.521). Hence, the larger size of the $T_1$6 tetrahedron is predicted by the population analysis. In addition, the $\langle T$–O$\rangle$ values recorded for the two Al-containing tetrahedra show the $T_2$6

Table 6. Observed tetrahedral bond lengths [$d(T$–O)Å], bond overlap populations [$n(T$–O)], geminal nonbonded overlap populations [$nb(T$–O)], the sum of the electrostatic bond strengths received by oxygen [ζ(O)], and the charges on the oxygen atoms as calculated by EHMO [Q(O)] for the Guildord (G) and White Well (WW) cordierites

Bond	$d(T$–O) WW	G	$n(T$–O) WW	G	$nb(T$–O) WW	G	ζ(O)	Q(O)
$T_1$1–$O_1$1	1.761	1.750	0.326	0.327	-0.0696	-0.0693	2.08	-1.40
$T_1$1–$O_1$3	1.754	1.756	.328	.329	-0.0695	-0.0694	2.08	-1.40
$T_1$6–$O_1$6	1.628	1.621	.518	.521	-0.0868	-0.0873	2.08	-1.38
$T_2$1–$O_2$1	1.586	1.583	.539	.545	-0.0745	-0.0755	1.75	-1.34
$T_2$1–$O_3$3'	1.606	1.603	.520	.524	-0.0809	-0.0848	2.00	-1.22
$T_2$1–$O_1$1	1.636	1.629	.512	.516	-0.0854	-0.0867	2.08	-1.39
$T_2$3–$O_2$6	1.574	1.568	.535	.537	-0.0743	-0.0752	1.75	-1.34
$T_2$3–$O_1$3	1.639	1.631	.513	.517	-0.0826	-0.0859	2.08	-1.39
$T_2$3–$O_2$3	1.614	1.619	.523	.524	-0.0850	-0.0880	2.00	-1.22
$T_2$6–$O_1$6	1.773	1.767	.334	.336	-0.0644	-0.0639	2.08	-1.39
$T_2$6–$O_2$6	1.710	1.719	.368	.368	-0.0577	-0.0574	1.75	-1.34
$T_2$6–$O_2$3	1.714	1.718	.366	.368	-0.0572	-0.0564	1.75	-1.34

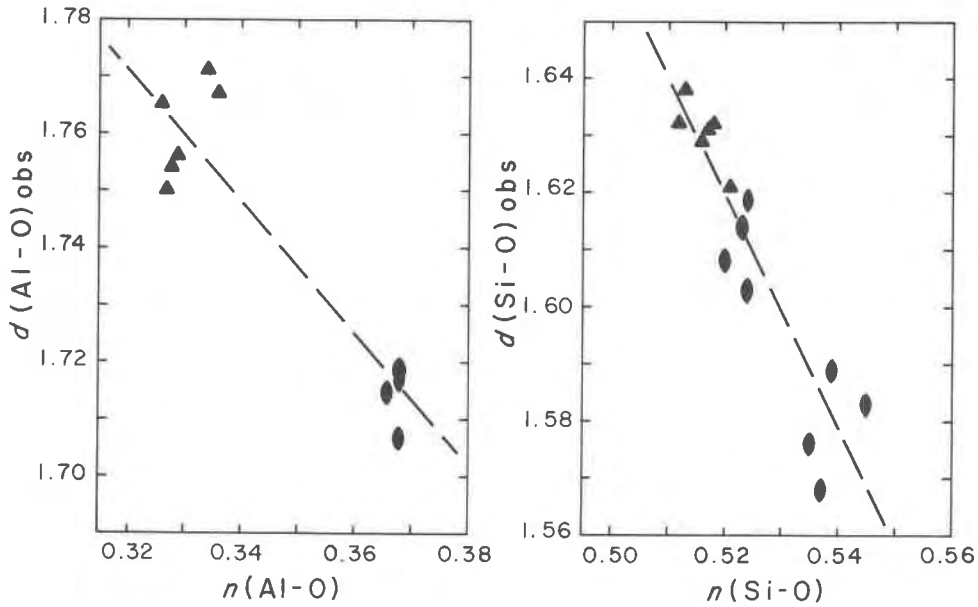

Fig. 3. Mulliken bond overlap populations, $n(T\text{–O})$, plotted against observed tetrahedral bond lengths, $d(T\text{–O})_{obs}$. In the calculation of $n(T\text{–O})$ for the tetrahedral framework, all bond lengths were clamped at 1.61 Å for SiO_4 tetrahedra and 1.75 Å for AlO_4 tetrahedra with observed angles maintained. The diad symbols refer to bonds involved in two-coordinated oxygen atoms, and the triad symbols refer to bonds involved in three-coordinated oxygen atoms. Data from Table 6.

tetrahedron to be significantly smaller (1.742 Å) than $T_1$1 (1.758 Å), suggesting a replacement of a small amount of Al by Si in $T_1$1. A comparison of the $\langle n(T\text{–O})\rangle$ and $\langle T\text{–O}\rangle$ values for these tetrahedra shows that the $\langle n(T\text{–O})\rangle$ value for the $T_2$6 tetrahedron (0.351) is larger than that for the $T_1$1 tetrahedron (0.327). Again we see that the apparent size discrepancy is predicted by the population analysis. Since

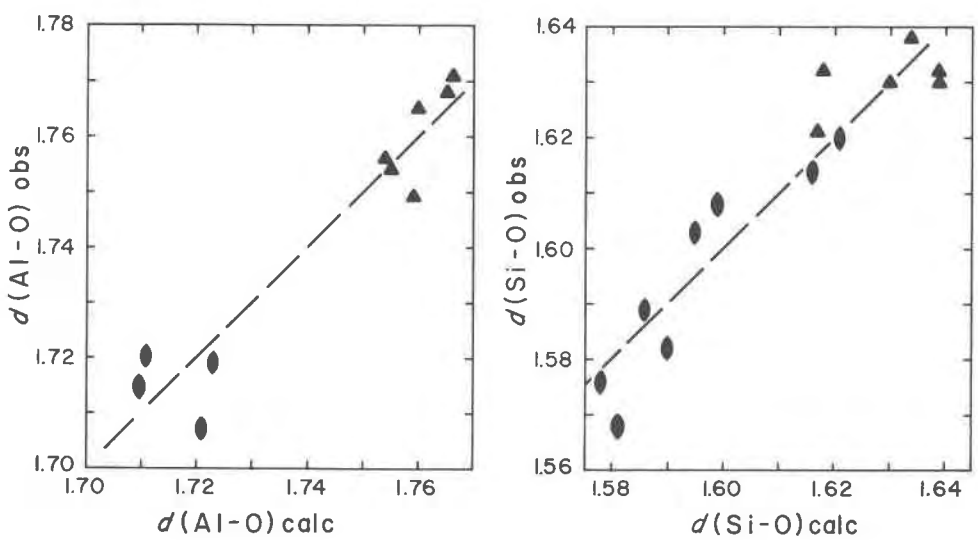

Fig. 4. Observed tetrahedral bond lengths, $d(T\text{–O})_{obs}$, plotted against the tetrahedral bond lengths, $d(T\text{–O})_{calc}$, calculated as a function of the mean tetrahedral angle, $\langle \text{O–}T\text{–O}\rangle_3$, and $-1/\cos(\angle\, T\text{–O–}T)$ where the equations of the lines are:

$$d(\text{Al–O})_{calc} = 2.544 + 0.055(-1/\cos(\angle\, T\text{–O–}T) - 0.008(\langle \text{O–Al–O}\rangle_3) \text{ and}$$

$$d(\text{Si–O})_{calc} = 2.915 + 0.035(-1/\cos(\angle\, T\text{–O–}T) - 0.012(\langle \text{O–Si–O}\rangle_3).$$

See Fig. 5 for explanation of symbols used.

the $n(T\text{–O})$ values are strongly dependent upon the T–O–T angles, theory predicts that tetrahedra with identical Al,Si contents should be larger when they are involved in T–O–T angles narrower than average. The structures of both the White Well and the Guilford cordierites are consistent with this prediction. A recent study of coesite (Gibbs *et al.*, 1976) shows that the larger of its two nonequivalent silicate tetrahedra is also involved in the narrower Si–O–Si angles. In addition, the mean Si–O bond overlap populations are consistent with the mean Si–O bond lengths:

tetrahedron	⟨Si–O⟩	⟨n(Si–O)⟩
Si1	1.601	0.504
Si2	1.612	0.501

In summary, it is apparent that caution should be exercised in concluding that the Al,Si contents of two tetrahedra are different just because their mean T–O bond lengths differ by ~0.01 Å; the environment around the tetrahedra may also be a factor.

Another parameter which may contribute to our understanding of the stereochemistry of the cordierite structure is the geminal nonbonding overlap populations, $nb(T\text{–O})$, which give a measure of the intramolecular forces that tend to stretch bonds (Bartell *et al.*, 1970) as the overlap populations decrease. The geminal nonbonded overlap populations for a bond may be calculated by taking the algebraic sum of all negative interactions around the bond as discussed in Figure 8. Since overlap populations were calculated only for the tetrahedral framework, the repulsion term for the octahedral cation M, $n(T\ldots M)$, was not included in our $nb(T\text{–O})$ values (Table 6). However, if $n(T\ldots M)$ were included, $nb(T\text{–O})$ would increase giving us a semiquantitative basis for the observation that bond lengths tend to increase as coordination number of the oxygen atom increases. For example, in cordierite, the T–O bonds involved with two-coordinated oxygens involve smaller repulsion terms and shorter bonds, whereas those involved with three-coordinated oxygens involve larger repulsion terms and longer bonds (Table 6). Despite the utter neglect in the calculations of the nontetrahedral cations, it is clear that smaller $n(T\text{–O})$ and larger $nb(T\text{–O})$ values were calculated for the T–O bonds to the three-coordinated oxygen atoms. This result agrees with the assertion that the valence angles observed within and between the tetrahedral ions incorporate part of the extrinsic effects of the nontetrahedral cations (Gibbs *et al.*, 1974). As expected, linear regression analysis for $d(T\text{–O})_{obs}$ calcu-

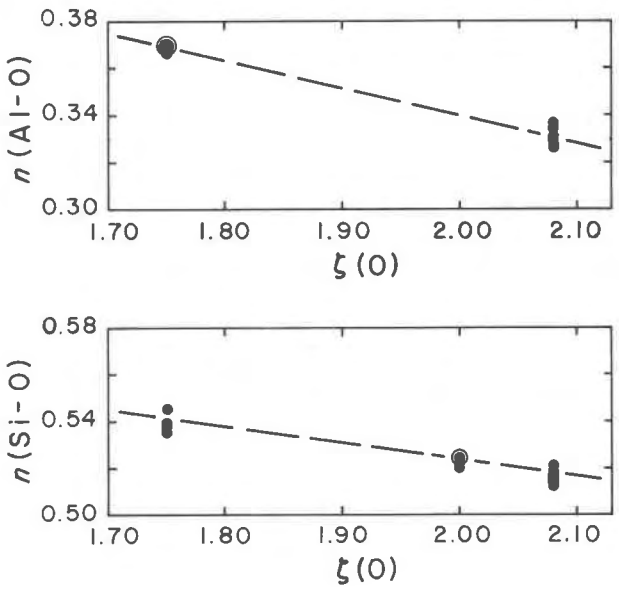

Fig. 5. Mulliken bond overlap populations, $n(T\text{–O})$, plotted against the sum of the electrostatic bond strengths received by oxygen, ζ(O). In the calculation of $n(T\text{–O})$ for the tetrahedral framework, all bond lengths were clamped at 1.61 Å for SiO_4 tetrahedra and 1.75 Å for SiO_4 tetrahedra with observed angles maintained. Data from Table 6.

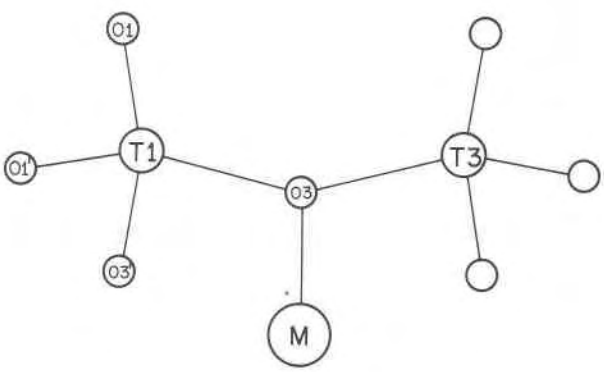

Fig. 6. Example calculation of the geminal nonbonded overlap population, $nb(T\text{–O})$, obtained by taking the algebraic sum of all nonbonded interactions across the bond as follows:

$$nb(T1\text{–}03) = n(03\ldots01) + n(03\ldots03') + n(03\ldots01') + n(T1\ldots T3) + n(T1\ldots M).$$

The nonbonded repulsion term involving the octahedral cation, $n(T\ldots M)$, is not included in the $nb(T\ldots O)$ values listed in Table 5, since overlap populations were calculated for the tetrahedral framework alone. However, it may be seen that inclusion of the nonbonded repulsions involving the M cation would increase the value of the nonbonded overlap population for the bonds to O3, predicting that T–O bonds to three-coordinated oxygens should be longer than those to two-coordinated oxygen atoms.

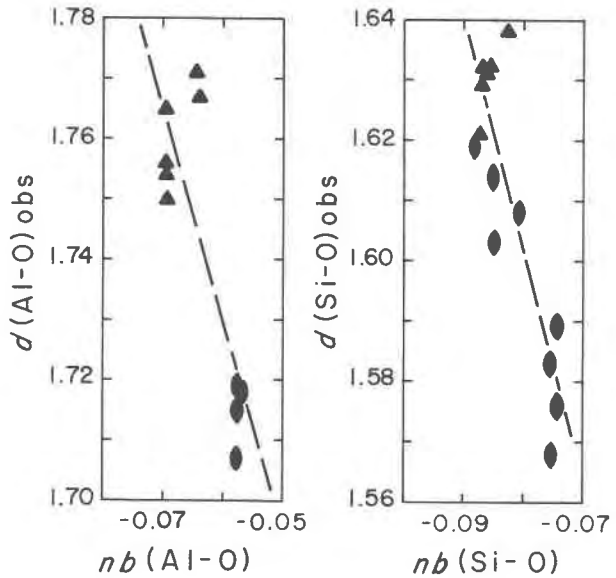

Fig. 7. Geminal (negative) nonbonded overlap populations, $nb(T\text{–O})$, plotted against the observed tetrahedral bond lengths, $d(T\text{–O})_{obs}$. A sample calculation of $nb(T\text{–O})$ is given in Fig. 6. Symbols are explained in Fig. 3, and data is from Table 6.

lated as a function of $[nb(T\text{–O})]$ show these correlations ($r = 0.8$) to be highly significant (Fig. 7).

Orientation of the water molecules

The orientation of the water molecule within the channels of cordierite was determined from X-ray and neutron $\Delta\rho$ maps (Cohen, 1975). The geometry of the water molecule [d(H1–Ow) = 1.04 Å, d(H2–Ow) = 0.97 Å, $\angle$ Hl–Ow–H2 = 102.4°] agrees reasonably well with an "idealized" H_2O geometry [d(H–O) ~1.0 Å, $\angle$ H–O–H = 104.5°]. The plane of the H_2O molecule lies closely parallel to (001) at z = 1/4. However, this result disagrees with the possible orientation of the molecule parallel to (100) as proposed by Farrell and Newnham (1967) for the Guilford cordierite and confirmed by Tsang and Ghose (1972) for a cordierite from Madagascar. The elongation of the peaks associated with Ow and H on X-ray and neutron $\Delta\rho$ maps is assumed to result from a space averaging of the disordered H_2O molecule in four different orientations occurring within the cavities throughout the crystal (Fig. 8). Figure 9 illustrates one of the four possible orientations in relation to the 6-membered rings above and below. In this orientation H2 is bonded to O_26 in the ring below, while H1 forms a weaker bond with O_21 in the ring above. This configuration may be rationalized in terms of EHMO electrical charges calculated for the oxygen atoms, Q(O), in the 6-membered rings where $Q(O_26) > Q(O_21) > Q(O_23)$ (Table 6). The H_2O molecule is then not totally disordered within the cavity but is oriented such that it forms the shortest bond with O_26, which has the largest electrical charge, and forms the longest bond with the O_23, which has the smallest electrical charge. Accepting Farrell and Newnham's (1967) possible orientation of H_2O in the channel, Stout (1975) has argued that the O_26 is pulled into the open channel because of its coordination with molecular water. Since the H_2O is quite loosely bound [d(H2–O_26) = 2.47 Å; d(H1–O_21) = 3.08 Å], it seems unlikely that electrostatic interactions of H_2O are responsible for a significant part of the bending of the T_26–O_26–T_23 angle.

Results of the neutron site refinement show no evidence for hydrogen replacing Si or Al in any tetrahedra in the framework, as suggested by Iiyama (1960) and Sugiura (1959). In addition, a neutron $\Delta\rho$ map calculated for the entire unit cell showed no large residual negative peaks attributable to hydrogen. A possible explanation for the rapid weight loss in cordierite above 500°C, from which Sugiura and

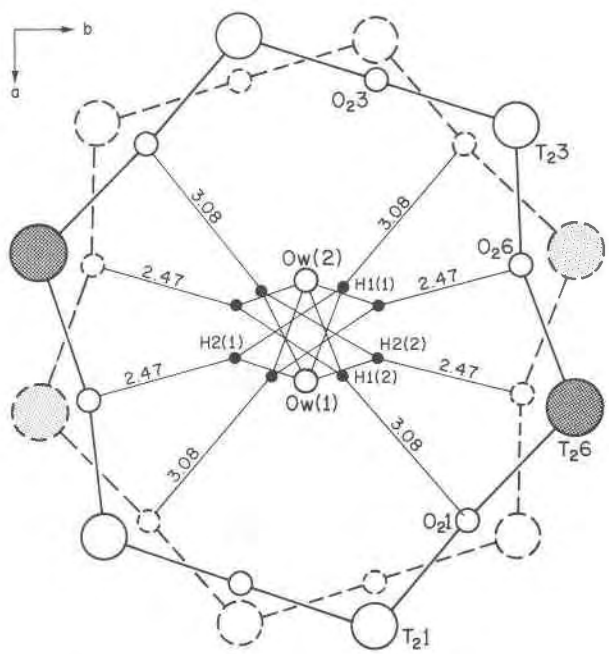

Fig. 8. Composite drawing of the four possible water molecule orientations in the channels of low cordierite. Elongation of the peaks associated with hydrogen in the y direction in neutron $\Delta\rho$ maps reflect this disordered model. Solid lines connect the 6-membered ring at $z = 0$ while dashed lines connect the 6-membered ring at $z = 1/2$. Shaded circles represent Al, large open circles represent Si, medium-sized open circles represent O and small solid circles represent H. Values indicated between H and O atoms refer to approximate bond lengths calculated from neutron diffraction data (Table 4).

Iiyama inferred the presence of tetrahedral hydrogen, may be the loss of alkaline atoms above 500°C.

X-ray and neutron $\Delta\rho$ maps confirm the location of the alkaline atoms at the center of the 6-membered rings as found by Meagher (1967) for the Haddam cordierite. However, elongation of the peak associated with the 0.09 alkaline atoms in the direction of the $O_2$6 oxygen in the 6-membered ring suggests that the alkaline atoms, like the water molecule, are disordered within the channel but oriented toward $O_2$6. Because of the small amounts of these atoms present in the White Well cordierite (0.63 weight percent), it was difficult to refine on a model for their occurrence. Nevertheless, the distances between the alkaline atoms at (0,0,0) and the O_2 oxygen atoms (Table 4) suggest possible electrostatic interactions between the alkaline atoms and $O_2$6, and between the alkaline atoms and Ow, which may influence the distribution of H_2O in the structure. A crystal structure analysis on a cordierite with a larger amount of alkaline atoms may provide more information on this subject and their possible role in the polymorphism of cordierite.

Orientation of the thermal ellipsoids

Tables 1, 2, and 3 compare the results of neutron (N) and X-ray (X) final positional and thermal parameters and interatomic distances and angles. The close agreement between positional parameters is characteristic of symmetric electron distributions about atoms. The differences in thermal parameters probably reflect the nonspherical nature of real electron distributions, which will be examined in a future study of X–N maps for the White Well cordierite. Table 5 shows the r.m.s. displacements of the atoms obtained from neutron and X-ray data to be similar. The disagreement of angular relationships for the thermal ellipsoids (Table 5) of the nearly spherically vibrating tetrahedral and octahedral atoms may be explained by the fact that the more spherical an ellipsoid becomes, the more ill-defined its orientation becomes. The axes of more elongate oxygen atoms are more easily defined, and agreement between the X and N data is improved. While the cations show little anisotropy, a stereographic plot of the thermal ellipsoids of oxygens in relation to the bonds in which they are involved show two trends.

(1) The two-coordinated O_2 oxygens in the ring vibrate as oblate spheroids with their short directions parallel to the *T*–O–*T* bonds and two long perpendicular thereto.

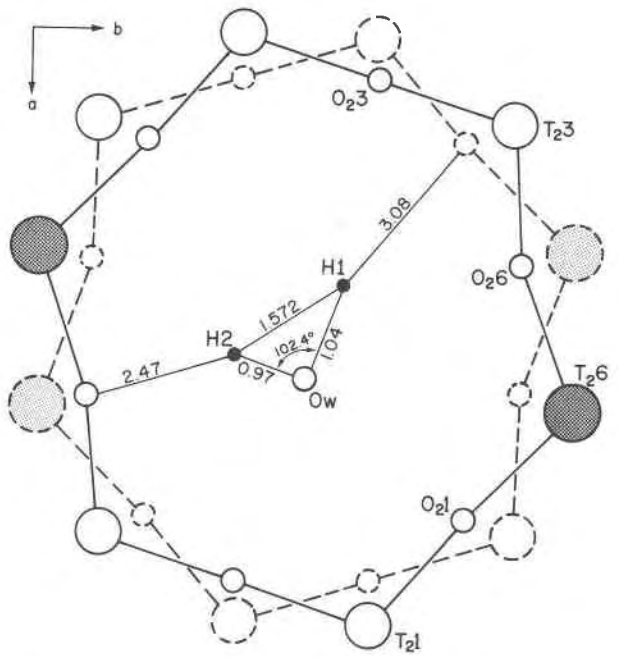

Fig. 9. Drawing of one of the four possible water molecule orientations located at the center of the cavity. The positions of Ow, H1 and H2 were determined by X-ray and neutron $\Delta\rho$ maps. In this example, H2 forms a bond with $O_2$6 in the ring below while H1 forms a weaker bond with $O_2$1 in the ring above. Symbols are explained in Fig. 8.

(2) The three-coordinated oxygens O_1 outside of the ring vibrate as prolate spheroids with their short r.m.s. displacements in the plane formed by coordination with Mg, Al, and Si and their long r.m.s. displacement approximately perpendicular thereto.

In other words, the oxygen atoms in cordierite vibrate about their equilibrium positions in conformity with the spatial requirements of their first coordination sphere of cations.

Acknowledgments

Professors F. D. Bloss, E. P. Meagher and P. H. Ribbe read the manuscript and made a number of valuable suggestions and constructive criticisms. We thank Mr. M. W. Pryce of the Government Chemical Laboratories, Perth, Western Australia, for donating the White Well cordierite, Mr. Elwin Yoder of the Argonne National Laboratories for cutting the cube of cordierite used in the neutron diffraction study, the Central Scientific Laboratory of Union Carbide Corporation, Tarrytown, New York, for the emission spectroscopic analysis for Be, Mr. A. Prunier for running a number of the EHMO calculations, Mrs. Ramonda Haycocks for typing the manuscript and Mrs. Sharon Chiang for drafting the figures. We are particularly grateful to Dr. Jack Williams for making available use of the Chemistry Division's single-crystal neutron diffractometer facilities at the CP-5 Reactor at the Argonne National Laboratories. This study was supported with N.S.F. grant DES75-14912.

References

Bartell L. S., L. S. Su and H. Yow (1970) Lengths of phosphorus-oxygen and sulfur-oxygen bonds. An extended Hückel molecular orbital examination of Cruickshank's d_π–p_π picture. *Inorg. Chem., 9,* 1903–1912.

Baur, W. H. (1970) Bond length variation and distorted coordination polyhedra in inorganic crystals. *Trans. Am. Crystallogr. Assoc. 6,* 125–155.

Brown, I. D. and R. D. Shannon (1973) Empirical bond-strength–bond-length curve for oxides. *Acta Crystallogr, A29,* 266–282.

Byström, A. (1942) The crystal structure of cordierite. *Ark. Kemi Mineral Geol., 15B* (No. 12), 1–5.

Cohen, J. P. (1975) *An X-ray and Neutron Diffraction Study of Hydrous Low Cordierite.* M. S. Thesis, Virginia Polytechnic Institute and State University, Blacksburg, Virginia.

———, F. K. Ross and G. V. Gibbs (1975) X-Ray and neutron diffraction study of low cordierite. (abstr.). *Abstr. Prog. 1975 Annu. Meet. Geol. Soc. Am., 7,* 1031.

Farrell, E. F. and R. E. Newnham (1967) Electronic and vibrational absorption spectra in cordierite. *Am. Mineral., 52,* 380–388.

Gibbs, G. V. (1966) The polymorphism of cordierite: I. The crystal structure of low cordierite. *Am. Mineral. 51,* 1068–1087.

———, S. J. Louisnathan, P. H. Ribbe and M. W. Phillips (1974) Semi-empirical molecular orbital calculations for atoms of the tetrahedral framework in anorthite, low albite, maximum microcline and reedmergerite. *In,* W. S. MacKenzie and J. Zussman, Eds., *The Feldspars.* Manchester University Press, Manchester. p. 49–67.

———, C. T. Prewitt and K. J. Baldwin (1976) A study of the structural chemistry of coesite. *Z. Kristallogr.,* in press.

Goldsmith, J. R. and F. Laves (1955) Cation order in anorthite ($CaAl_2Si_2O_8$) as revealed by gallium and germanium substitutions. *Z. Kristallogr, 106,* 213–226.

Gossner, B. and F. Mussgnug (1928) Vergleichende röntgenographische Untersuchung von Magnesiumsilikaten. *Neues Jahrb. Mineral., A58,* 213–252.

Iiyama, T. (1960) Recherches sur le role de l'eau dans la structure et la polymorphisme de la cordierite. *Bull. Soc. Fr. Mineral., 83,* 155–178.

Loewenstein, W. (1954) The distribution of aluminum in the tetrahedra of silicates and aluminates. *Am. Mineral., 39,* 92–96.

Meagher, E. P. (1967) *The Crystal Structure and Polymorphism of Cordierite.* Ph.D. Thesis, The Pennsylvania State University, University Park, Pennsylvania.

Newton, R. C. (1966) BeO in pegmatitic cordierite. *Mineral. Mag., 35,* 920–927.

———(1972) An experimental determination of the high-pressure stability limits of magnesium cordierite under wet and dry conditions. *J. Geol., 80,* 398–420.

Pauling, L. (1960) *The Nature of the Chemical Bond.* 3rd ed. Cornell University Press, Ithaca, New York.

Phillips, M. W., P. H. Ribbe and G. V. Gibbs (1973) Tetrahedral bond length variation in anorthite. *Am. Mineral., 58,* 495–499.

Pryce, M. W. (1973) Low-iron cordierite in phlogopite schist from White Well, Western Australia. *Mineral. Mag., 39,* 241–243.

Schreyer, W. and H. S. Yoder (1964) The system Mg–cordierite–H_2O and related rocks. *Neues Jahrb. Mineral. Abhand. 101,* 271–342.

Smith, J. V. and S. W. Bailey (1963) Second review of Al–O and Si–O tetrahedral distances. *Acta Crystallogr., 16,* 801–811.

———and W. Schreyer (1960) Location of argon and water in cordierite. *Mineral. Mag., 33,* 226–236.

Stout, J. (1975) Apparent effects of molecular water on the lattice geometry of cordierite. *Am. Mineral., 60,* 229–234.

Strunz, H., C. Tennyson and P.-J. Uebel (1971) Cordierite morphology, physical properties, structure, inclusions and oriented intergrowth. *Minerals Science and Engineering,* April 1971, 3–18.

Sugiura, K. (1959) The water problem of cordierite. *Bull. Tokyo Inst. Tech.,* Ser. B. *1,* 1–26.

Takane, K. and T. Takeuchi (1936) The crystal structure of cordierite. *Jap. Assoc. Mineral. Petrol. Econ. Geol. J., 116,* 101–127 (in Japanese).

Tsang, T. and S. Ghose (1972) Nuclear magnetic resonance of ^1H and ^{27}Al and Al–Si order in low cordierite, $Mg_2Al_4Si_5O_{18}\cdot nH_2O$. *J. Chem. Phys., 56,* 3329–3332.

Zoltai, T. (1960) Classification of silicates and other minerals with tetrahedral structures. *Am. Mineral., 45,* 960–973.

Manuscript received, February 1, 1976; accepted for publication, July 16, 1976.